

# A 2D-3D simplified modeling strategy to simulate the non linear behavior of U-shaped walls

P.Kotronis, L.Davenne & J.Mazars

Laboratoire de Mécanique et de Technologie, 61 avenue du Président Wilson, 94235 Cachan cedex, France

**ABSTRACT:** Within the framework of the TMR - ICONS research program, dynamic and cyclic tests on U-shaped shear walls have been performed at CEA Saclay and JRC Ispra respectively. The paper presents the simulations made at LMT Cachan in order to prepare the tests and the comparisons between the numerical and the experimental results. 2D multi-layered Bernoulli beam elements and uniaxial constitutive laws based on damage mechanics and plasticity have been used to define the seismic intensity levels to be applied during the shaking-table tests. In order to simulate the cyclic tests a 3D multifiber Timoshenko beam element with higher order interpolation functions has been developed. Comparison with the experimental results shows the well funding and the limitations of the two approaches.

## 1 INTRODUCTION

Within the framework of the of the 5<sup>th</sup> topic ("Shear Wall Structures") of the TMR (Training and Mobility of Researchers) ICONS ("Innovative Seismic Design Concepts for New and Existing Structures") European Program, a series of dynamic and cyclic tests on U-shaped cross section shear walls have been made at CEA Saclay (Combesure et al. 1999) and at JRC Ispra (Pegon et al. 2000) respectively. The tests have been performed until collapse of the structures. By collapse we mean the appearance of significant cracks on the concrete walls and significant plastic strain with possible failure of some bars of the vertical reinforcing steel. The purpose of this paper is to present the calculations done in Laboratoire de Mécanique et de Technologie (LMT) in order to prepare the tests and the comparison between numerical and experimental results.

We begin with the presentation of the dynamic tests at CEA Saclay and the description of the specimens. As the loading was uniaxial and parallel to the flanges a 2D simplified model was chosen for the preliminary calculations. The 2D multi-layered Bernoulli beam elements of the code EFICOS and 1D constitutive laws based on damage mechanics and plasticity are used to simulate the non linear behavior of the mock-ups. The calculations helped to define the loading and the seismic intensity levels to be applied during the test.

For the cyclic test at JRC Ispra the loading was bi-directional and 3D phenomena were prevailing. In

order to simulate the non linear behavior of the specimens a 3D multifiber Timoshenko beam element has been implemented into the library FEDEAS (Filippou 1996) of the finite element code FEAP (Taylor 1996). The element is valid for arbitrarily sections and uses higher order interpolation functions to avoid shear locking phenomena. Comparison with the experimental results shows the ability of the model to reproduce the behavior of the mock-ups.

## 2 SHAKING TABLE TESTS

### 2.1 Description of the specimens

4 U-shaped walls have been tested on the Azalée shaking table of the EMSI Laboratory at CEA Saclay (Combesure et al. 1999). The walls have been designed according to the Eurocode 8 (EC8), they are geometrically identical and they have the same flexural reinforcement. The spacing of the stirrups is the only difference between the specimens. The aim of the tests was to study the difference in the seismic behavior due to the stirrups spacing.

The 0.60 scale mock-up is composed of the U-shaped wall itself, an inferior slab at the base of the wall and a superior slab at the top where additional masses are fixed (Fig. 1). In order to define the properties of the materials, compressive and tensile tests have been performed on concrete and steel specimens respectively. The walls have been instru-

mented to monitor their global (displacements, accelerations) and local (crack openings, strains of the steel reinforcement, shear deformation) behavior.

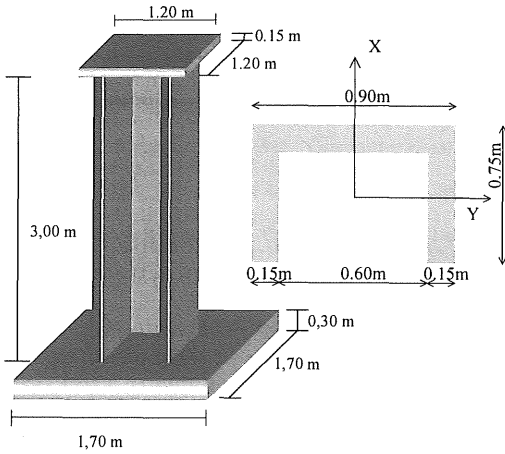


Figure 1. Dynamic test - Description of the specimens.

## 2.2 Description of the loading

An artificial accelerogram has been generated to match the EC8 reference elastic spectrum and it was contracted with a scale factor of  $0.6^{1/2}$  (0.6 being the scale of the mock-up). With this similitude law, the acceleration remains unchanged but the time scale is contracted in order to reduce the displacement (Fig. 2). Increasing levels of a signal proportional to this artificial accelerogram were to be applied at the X direction, parallel to the flanges of the specimens. In order to define the loading sequences and the "failure" acceleration the following predictive non linear numerical studies were performed at LMT.

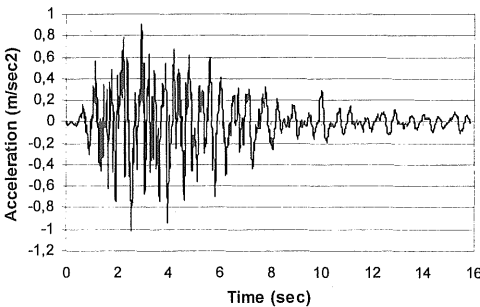


Figure 2. Dynamic test – Generated artificial accelerogram.

## 2.3 Predictive numerical studies

### 2.3.1 Finite element mesh

For the 2D calculations presented in this paper, the code EFICOS, developed at LMT, was used. 30

Bernoulli multi-layered beam elements having a T section model the shear wall (Fig. 3). Each beam is divided into 31 layers. The inferior slab is considered elastic and the wall is fixed at the base. The seismic table is introduced via a rigid beam resting upon three linear springs.

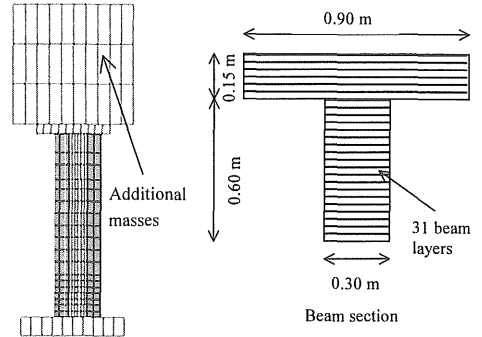


Figure 3. Dynamic test – EFICOS mesh.

### 2.3.2 Constitutive models

1D constitutive laws for concrete and steel are applied at each layer. Seismic loading, which includes cyclic aspects, produces micro-cracking in concrete. The major phenomena – decrease in material stiffness as the micro-cracks open, stiffness recovery as the cracks close (unilateral behavior of concrete) and inelastic strains concomitant to damage – have to be taken into account. The constitutive law used for concrete is based on the principles of damage mechanics (La Borderie 1991). The law, called "Unilateral damage law", is elaborated for the description of micro-cracks, involves two damage scalar variables one in tension and one in compression and the description of isotropic inelastic strains. The model is able to simulate the unilateral behavior of concrete via a recovery stiffness procedure at re-closure. The total strain in the 3D formulation of the law is given by:

$$\varepsilon = \varepsilon^e + \varepsilon^m \quad (1)$$

$$\varepsilon^e = \frac{\langle \sigma \rangle_+}{E(1-D_1)} + \frac{\langle \sigma \rangle_-}{E(1-D_2)} + \frac{\nu}{E}(\sigma - \text{Tr}(\sigma))\mathbf{I} \quad (2)$$

$$\varepsilon^m = -\frac{\beta_1 D_1}{E(1-D_1)} \frac{\partial f(\sigma)}{\partial \sigma} + \frac{\beta_2 D_2}{E(1-D_2)} \mathbf{I} \quad (3)$$

where  $\varepsilon^e$  = elastic strain tensor;  $\varepsilon^m$  = inelastic strain tensor;  $\mathbf{I}$  = unit tensor; and  $\text{Tr}(\sigma) = \sigma_{ii}$ . Damage criteria are expressed as:

$$f_i = Y_i - Z_i \quad (4)$$

$Y_i$  associates forces to damage; and  $Z_i$  threshold depending on the hardening variables. The evolution law for damage takes the form:

$$D_i = I - \frac{1}{1 + [A_i(Y_i - Y_{0i})]^{\beta_i}} \quad (5)$$

$$\begin{cases} Tr(\sigma) \in [0, +\infty] \rightarrow \frac{\partial f(\sigma)}{\partial \sigma} = 1 \\ Tr(\sigma) \in [-\sigma_f, 0] \rightarrow \frac{\partial f(\sigma)}{\partial \sigma} = \left(1 - \frac{Tr(\sigma)}{\sigma_f}\right) I \\ Tr(\sigma) \in [-\infty, -\sigma_f] \rightarrow \frac{\partial f(\sigma)}{\partial \sigma} = 0. I \end{cases} \quad (6)$$

$f(\sigma)$  = crack closure function;  $\sigma_f$  = crack closure stress respectively;  $\langle \cdot \rangle_+$  denotes the positive part of a tensor;  $E$  = initial Young's modulus;  $\nu$  = Poisson ratio;  $D_1$  and  $D_2$  = damage variables for traction and compression respectively.  $Y_{0i}$  = initial elastic threshold ( $Y_{0i} = Z_i(D_i=0)$ ); and  $A_i, B_i, \beta_1, \beta_2$  = material constants.

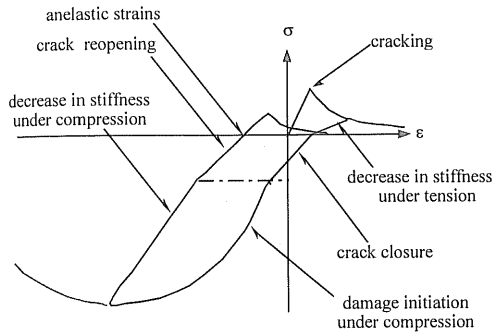


Figure 4. 1D "Unilateral damage law".

For the numerical calculations the mean compression strength is taken equal to 30 MPa and the elastic Young modulus 28 GPa. Confinement is not taken into account.

A plasticity model with cinematic hardening is used for steel. Hardening can be linear or not depending on the information provided from the steel tensile strength tests. The stress-strain relation is given Figure 5. Only the longitudinal reinforcement is considered for the predictive calculations. It is introduced with special layers, the behavior of which is a combination of those of concrete and of steel (Mazars 1998). Shear reinforcement and stirrups are not simulated. The yield strength is taken equal to 500 MPa and the Young modulus 200 GPa.

Damping is introduced in the analysis through viscous forces generated by a global damping matrix. This matrix is taken as a linear combination of

the global stiffness matrix and the mass matrix (Rayleigh damping). 2% damping was chosen for the first mode and 4% for the second. Damping stays constant during the calculation.

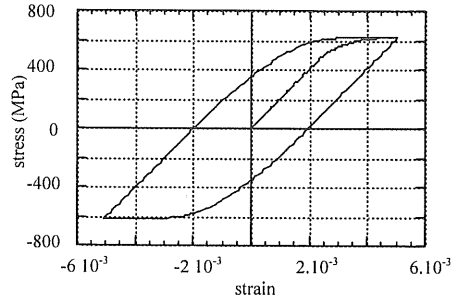


Figure 5. 1D steel constitutive law.

### 2.3.3 Results

The accelerogram of Figure 2 is applied to the numerical model of Figure 3 in the X direction following an increasing level sequence. The maximum values of the global and local results are shown in Table 1.

Table 1. Results of the predictive calculations

|                                  | 0.20g | 0.60g | 0.80g | 1.0g |
|----------------------------------|-------|-------|-------|------|
| Displacement at the top (cm)     | 1.39  | 3.95  | 5.49  | 5.91 |
| Bending moment at the base (KNm) | 334   | 437   | 465   | 504  |
| Steel strain at the base (%)     | 0.04  | 1.1   | 1.6   | 2.4  |

Yielding of steel starts for a level between 0.2g and 0.6g ( $\epsilon_{sy}=0.25\%$ ). At 0.6g we reach the ultimate steel deformation ( $\epsilon_{sd}=1\%$ ). Finally at 1.0g we have some steel bars broken ( $\epsilon_{su}=2.5\%$ ).

Predictive calculations showed also a dynamic variation of the axial force at the base of the wall. As the cracks close, shock is induced, stiffness changes suddenly and the pumping mode of the mock-up is excited. This variation of the vertical dynamic forces is important and for more some sequences it can almost double or cancel the dead weight of the mock-up.

This study, together with other predictive calculations made by CEA Saclay et INSA de Lyon (Manas et al. 1999), confirmed the basic characteristics of the non linear behavior of the mock-ups and helped to define the following loading history during the tests:

- A low level test (0.25g) with no or few yielding of the vertical steel bars
- A medium level test (0.60g) with moderate yielding
- High test up to the failure of the wall (1.0g).

After the tests however, this 2D model was proved inadequate to reproduce correctly the experimental results for high levels of acceleration. Due to its simplified assumptions (confinement and stirrups are not considered, T instead of U section), it failed to simulate the displacement or the bending moment time history for 1.0g. In order to study the influence of stirrups at the non linear behavior of the 4 specimens a multifiber element must instead be used. With such an element we can not only discretize exactly the section of the walls but also introduce the influence of the confinement by changing the properties of concrete in the appropriate fibers.

### 3 CYCLIC TEST

#### 3.1 Description of the specimen

4 U-shaped walls have been tested in the reaction wall facility of the ELSA laboratory at JRC Ispra (Pegon et al. 2000). The 1.0 scaled specimens are composed of the U-shaped wall itself, the inferior slab and the superior slab and they all have the same dimensions and steel reinforcement (Figs 6-7). The superior slab is used as the horizontal load application point. 6 vertical post-tensioning bars apply the normal force (2MN). These bars are disposed in a way that the force is applied close to the inertial cen-

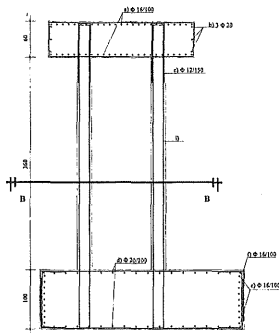


Figure 6. Cyclic test – Description of the specimen.

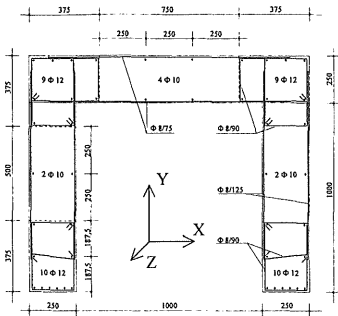


Figure 7. Cyclic test – Section of the specimen.

ter in order to avoid spurious bending on the structure. Torsion is prohibited during the tests. The walls have been instrumented in order to monitor their global (displacements, accelerations) and local (crack openings, strains of the steel reinforcement, shear deformation) behavior.

#### 3.2 Description of the loading

The third test of the program is detailed hereafter. In contrast with the previous ones, where uniaxial load was used, the wall is loaded in both directions according to the butterfly path presented in Figure 8 (Pegon et al. 2000).

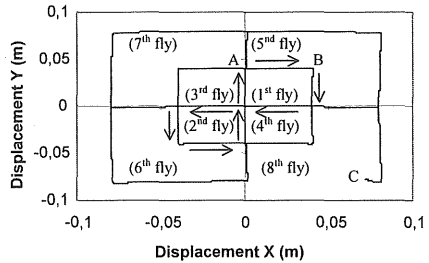


Figure 8. Cyclic test – Butterfly path.

#### 3.3 Numerical simulation of the test

##### 3.3.1 A multifiber Timoshenko beam element

In order to model the test, a 3D multifiber Timoshenko beam element has been developed (Kotronis 2000). The element uses higher order interpolation functions to avoid any shear locking phenomena (Friedman & Kosmatka 1993). For simplicity reason they are presented hereafter for a 2D element:

$$\begin{Bmatrix} u_s(x) \\ v_s(x) \\ \theta_s(x) \end{Bmatrix} = \begin{bmatrix} h_1 & 0 & 0 & h_2 & 0 & 0 \\ 0 & h_3 & h_4 & 0 & h_5 & h_6 \\ 0 & h_7 & h_8 & 0 & h_9 & h_{10} \end{bmatrix} \begin{Bmatrix} u_1 \\ v_1 \\ \theta_1 \\ u_2 \\ v_2 \\ \theta_2 \end{Bmatrix} \quad (7)$$

where  $s$  defines the “generalized” displacements and  $h$  the interpolations functions (8). These interpolations functions depends on the materials properties and they are calculated only once, for the first in-

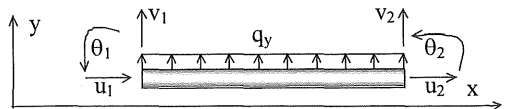


Figure 9. 2D Timoshenko beam element

crement. They are made interdependent by requiring them to satisfy the homogeneous differential equations associated with Timoshenko's beam theory. The variable  $\phi$  (9) is the ratio of the beam bending stiffness to the shear stiffness. For slender structures  $\phi$  equals zero and the resulting stiffness and mass matrices are reduced to matrices for the Bernoulli-Euler beam theory.

$$\left\{ \begin{aligned} h_1 &= 1 - \frac{x}{L} \\ h_2 &= \frac{x}{L} \\ h_3 &= \frac{1}{1+\phi} \left\{ 2\left(\frac{x}{L}\right)^3 - 3\left(\frac{x}{L}\right)^2 - \phi\left(\frac{x}{L}\right) + 1 + \phi \right\} \\ h_4 &= \frac{L}{1+\phi} \left\{ \left(\frac{x}{L}\right)^3 - \left(2 + \frac{\phi}{2}\right)\left(\frac{x}{L}\right)^2 + \left(1 + \frac{\phi}{2}\right)\left(\frac{x}{L}\right) \right\} \\ h_5 &= -\frac{1}{1+\phi} \left\{ 2\left(\frac{x}{L}\right)^3 - 3\left(\frac{x}{L}\right)^2 - \phi\left(\frac{x}{L}\right) \right\} \\ h_6 &= \frac{L}{1+\phi} \left\{ \left(\frac{x}{L}\right)^3 - \left(1 - \frac{\phi}{2}\right)\left(\frac{x}{L}\right)^2 - \frac{\phi}{2}\left(\frac{x}{L}\right) \right\} \\ h_7 &= \frac{6}{(1+\phi)L} \left\{ \left(\frac{x}{L}\right)^2 - \left(\frac{x}{L}\right) \right\} \\ h_8 &= \frac{1}{1+\phi} \left\{ 3\left(\frac{x}{L}\right)^2 - (4+\phi)\left(\frac{x}{L}\right) + (1+\phi) \right\} \\ h_9 &= -\frac{6}{(1+\phi)L} \left\{ \left(\frac{x}{L}\right)^2 - \left(\frac{x}{L}\right) \right\} \\ h_{10} &= \frac{1}{1+\phi} \left\{ 3\left(\frac{x}{L}\right)^2 - (2-\phi)\left(\frac{x}{L}\right) \right\} \end{aligned} \right. \quad (8)$$

$$\phi = \frac{12}{L^2} \left( \frac{EI}{kGA} \right) = \frac{24}{L^2} \left( \frac{I}{kA} \right) (1+\nu) \quad (9)$$

where  $L$  = length of the beam;  $A$  = section of the beam;  $\nu$  = Poisson's coefficient;  $k$  = shear correction factor;  $G$  = shear modulus;  $E$  = Young's modulus;  $I$  = area moment of inertia of the cross section.

The section constitutive matrix for the 3D formulation of the element and for non homogeneous section takes the form (Guedes et al. 1994):

$$K_s = \begin{bmatrix} K_{s11} & 0 & 0 & 0 & K_{s15} & K_{s16} \\ & K_{s22} & 0 & K_{s24} & 0 & 0 \\ & & K_{s33} & K_{s34} & 0 & 0 \\ & & & K_{s44} & 0 & 0 \\ & & & & K_{s55} & K_{s56} \\ \text{sym} & & & & & K_{s66} \end{bmatrix} \quad (10)$$

$$K_{s11} = \int_G EdS; \quad K_{s15} = \int_G EzdS;$$

$$K_{s16} = -\int_G EydS; \quad K_{s22} = k_y \int_G GdS$$

$$K_{s24} = -k_y \int_G GzdS; \quad K_{s33} = k_z \int_G GdS;$$

$$K_{s34} = k_z \int_G Gy dS; \quad K_{s44} = \int_G G(k_z y^2 + k_y z^2) dS$$

$$K_{s55} = \int_G Ez^2 dS; \quad K_{s56} = -\int_G Eyz dS;$$

$$K_{s66} = \int_G Ey^2 dS$$

( $E$  and  $G$  are functions of  $y$  et  $z$ ).

### 3.3.2 Results

11 multifiber Timoshenko beam elements are used to model the wall. 177 fibers simulates concrete and 46 fibers steel. Two gauss points are considered at each element. Base slab is not simulated and the wall is considered fixed at the base. Superior slab is linear and rotation of the upper part is prohibited in order to correctly reproduce the boundary conditions of the test.

1D constitutive laws are used for concrete and steel (Fig. 4-5). Specific values used for the materials are presented Table 2.

Table 2. Specific values used for the materials

|  |            |
|--|------------|
| Young's modulus (concrete)               | 20000 MPa  |
| Poisson coefficient (concrete)           | 0.2        |
| Compression strength (concrete)          | 31 MPa     |
| Compression strength (confined concrete) | 39 MPa     |
| Young's modulus (steel)                  | 200000 MPa |
| Poisson coefficient (steel)              | 0.3        |
| Yield strength (steel)                   | 460 MPa    |
| Ultimate strength (steel)                | 710 MPa    |
| Ultimate deformation (steel)             | 11%        |

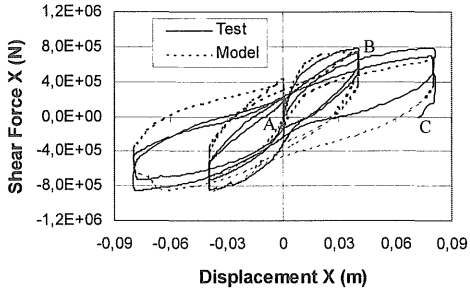


Figure 10. Cyclic test – Displacement and shear force in the X direction. Comparison test model.

Comparison of the numerical and experimental results for the eight flies of loading is represented at Figures 10-11 (the A,B,C letters refer to the Figure 8). The model simulates correctly the global behavior of the mock-up in terms of displacements in both directions. Calculation is not time consuming and allows for parametrical studies. Results can be improved by considering non linear shear behavior via 2D and 3D robust constitutive models for concrete.

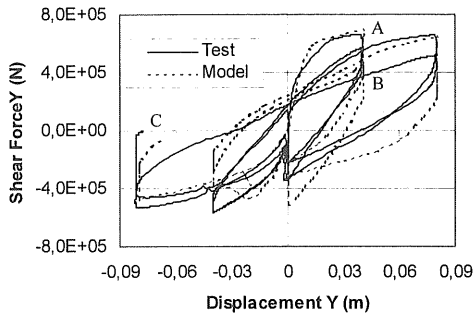


Figure 11. Cyclic test – Displacement and shear force in the Y direction. Comparison test model.

#### 4 CONCLUSIONS

Within the framework of the TMR ICONS European program the non linear behavior of U shaped reinforced concrete walls has been studied. Specimens have been tested dynamically on the largest shaking table in Europe at CEA Saclay and statically in the reaction wall facility of the ELSA laboratory at JRC Ispra. The U shaped walls have been designed in accordance with Eurocode 8 and loaded in one or two directions until collapse.

Numerical calculations during both pre-experimental and post-experimental phases have been made at LMT. The work continues onto the research already made in LMT in order to develop simplified models for computing concrete structures in non-linear dynamics. For the 2D calculations we have used the finite element code EFICOS. The mock-ups are simulated with 2D multi-layered Bernoulli beam elements and constitutive laws based on damage mechanics and plasticity. Predictive calculations helped to define the loading sequences and the maximum acceleration to apply to the structures. Comparison with the experimental results showed however the limitations of such approach for high intensity levels.

A new multifiber 3D beam element was developed in order to simulate the out of plane behavior of the specimens. The two-node displacement based element has a Timoshenko cinematic and takes into account the shear strain due to flexion. To avoid shear locking problems specific shape functions depending on the material characteristics have been used. Comparison between the experimental and the numerical results shows the efficiency of the new modeling tool to simulate the global behavior of the U shaped structural walls.

The proposed 2D and 3D models are non-time consuming and allow for parametrical studies even though the phenomena are quite complex. This paper proposes an overview of this work which, at the same time, opens the field of the treatment of torsion effects for asymmetric structures.

#### REFERENCES

- Combescur D., Chaudat Th., & Moutafidou A. 1999. Seismic tests of ICONS U-shaped walls. Description of the experimental set up. Main results. *Rapport DMT, SEMT/EMSI/RT/99-062*, CEA Saclay.
- Filippou F.C. 1996. Nonlinear static and dynamic analysis for evaluation of structures. *3<sup>rd</sup> European Conference on Structural Dynamics Eurodyn 96*, Florence Italy, 395-402.
- Friedman Z. & Kosmatka J.B. 1993. An improved two-node Timoshenko beam finite element. *Computers and structures*, Vol. 47, no 3, pp. 473-481.
- Guedes J., Pégon P & Pinto A. 1994. A fibre Timoshenko beam element in CASTEM 2000. *Special publication Nr. 1.94.31, JRC, I-21020 Ispra, Italy*.
- Kotronis P. 2000. Cisaillement dynamique de murs en béton armé. Modèles simplifiés 2D et 3D. *Ph.D. thesis, ENS Cachan*.
- La Borderie C. 1991. Phénomènes unilatéraux dans un matériau endommageable: modélisation et application à l'analyse des structures en béton. *Ph.D, Université Paris 6*.
- Manas B., Jeanvoine E. & Combescur D. 1998. Etude du comportement à la ruine d'une structure à murs porteurs en béton armé. *Report DMT-SEMT/EMSI/RT/98-068A*.
- Mazars J. 1998. French advanced research on structural walls : An overview on recent seismic programs. *Proc. 11<sup>th</sup> European Conference on Earthquake Engineering, Opening lecture*; edit. Ph. Bisch et al. Balkema Rotterdam, 21-41, Paris.
- Pegon P., Plumier C., Pinto A., Molina J., Gonzalez P., Tognoli P., & Hubert O. 2000. Quasi-static bi-axial test in the X and Y directions-Test report. June, *JRC Ispra*.
- Taylor R.L. 1996. FEAP: A finite element analysis program, version 5.01 manual. *University of California, Berkeley*.